CHEMICAL ENGINEERING TRANSACTIONS
VOL. 103, 2023
A publication of AIDIC
The Italian Association of Chemical Engineering
Online at www.cetjournal.it
Guest Editors: Petar S. Varbanov, Panos Seferlis, Yee Van Fan, Athanasios Papadopoulos

ISBN 979-12-81206-02-1; **ISSN** 2283-9216
DOI: 10.3303/CET23103080

CFD Aided Investigation of a Small Horizontal Wind Turbine Performance Enhancement Using Riblets

Chris Bliamis[a], Zinon Vlahostergios[b,*], Dimitrios Misirlis[c], Kyros Yakinthos[a]

[a]Laboratory of Fluid Mechanics and Turbomachinery, Department of Mechanical Engineering, Aristotle University of Thessaloniki, 54124 Thessaloniki, Greece
[b]Laboratory of Fluid Mechanics and Hydrodynamic Machines, Department of Production and Management Engineering, Democritus University of Thrace, 67100 Xanthi, Greece
[c]Department of Mechanical Engineering, International Hellenic University, 62124 Serres, Greece
zvlachos@pme.duth.gr

In recent years, the total number of wind turbines operating globally has steadily increased due to the relatively high technological readiness level and relatively low environmental footprint. An additional boost in this trend is expected in the near future, as costs of other “green” energy sources (i.e. natural gas) are rapidly rising. In the present work, the performance enhancement of a small horizontal wind turbine (SHWT) is examined by applying riblet geometries. The SHWTs typically have a disk blade radius of 1.5 to 3.5 m and a hub height of about 15m and operate inside the atmospheric boundary layer in high turbulence conditions. The use of riblets aims at reducing the turbine blade’s skin friction drag by altering the boundary layer characteristics in the near wall region and increasing the SHWT’s efficiency. More specifically, CFD computations are performed on the SHWT, by solving the steady RANS equations, along with the two-equation k-ω SST eddy viscosity turbulence model. The presence of riblets in the boundary layer region is modelled as transitional roughness and is implemented on the SHWT by using a dedicated boundary condition for the specific turbulence dissipation rate transport equation. The drag reduction and power output gain of the overall SHWT is estimated to be around 8 % and 1.5 % for the application of optimal-sized riblets.

1. Introduction

Wind turbines have emerged as a leading source of renewable energy production, with their adoption accelerating globally due to their environmentally friendly and cost-effective nature. Wind power capacity is expected to grow annually by around 110 GW until 2026, reaching well over 1,000 GW worldwide and making up a significant portion of the total energy mix (GWEC, 2022). While large horizontal-axis wind turbines (HAWTs) are currently dominant, small horizontal wind turbines (SHWTs) have gained increasing interest mainly due to their lower installation costs, reduced environmental impact, and suitability for off-grid and remote locations installation. They are usually much smaller than traditional wind turbines, with rotor diameters typically in the range of a few meters. SHWTs are often used in residential or small commercial settings where there is a need for localised power generation and can also act supplementary to other existing power sources (KC et al., 2019). As such, research into SHWTs has expanded in recent years, with a focus on improving their efficiency, reducing their cost, and increasing their reliability, both by employing innovative design choices as well as various flow control techniques.

One possible passive flow control technique that is examined on wind turbines is the use of riblets, which are small, regularly spaced groove geometries in the order of a few hundred μm, inspired by the skin of sharks. The riblets reduced the skin friction of turbulent boundary layers by interacting with the small-scale vortical structures in the near wall region (García-Mayoral and Jiménez, 2011). Specifically, they alter the flow inside the boundary layer with three distinct mechanisms: (a) by elevating the cross-flow motion in their crests upwards and displacing streamwise vortices and streaks away from the wall, (b) by weakening the near-wall turbulence regeneration cycle and (c) by dampening the spanwise flow fluctuations (Bannier et al., 2015). However, they also amplify the two-dimensional Tollmien–Schlichting waves, and inappropriately designed or placed riblets

Paper Received: 13 April 2023; Revised: 09 June 2023; Accepted: 28 June 2023
Please cite this article as: Bliamis C., Vlahostergios Z., Misirlis D., Yakinthos K., 2023, CFD Aided Investigation of a Small Horizontal Wind Turbine Performance Enhancement Using Riblets, Chemical Engineering Transactions, 103, 475-480 DOI:10.3303/CET23103080

can result in a drag increase as they promote the laminar to turbulent boundary layer transition (Klumpp et al., 2010). The basic geometric parameters which define riblets are presented for blade-shaped riblets in Figure 1a, and more specifically, the groove width s, height h, thickness t, and groove cross-section A_g. These geometric characteristics are usually given in wall units (s^+, h^+, l_g^+) to allow the easy comparison between different experiments. Based on a large number of experimental works, it has been demonstrated that riblets operate optimally, and provide the greatest drag reduction, for $s^+ \approx 15$ and $l_g^+ \approx 10.5$ (Figure 1b), with the latter being a better indicator of their performance (Garcia-Mayoral and Jimenez, 2011).

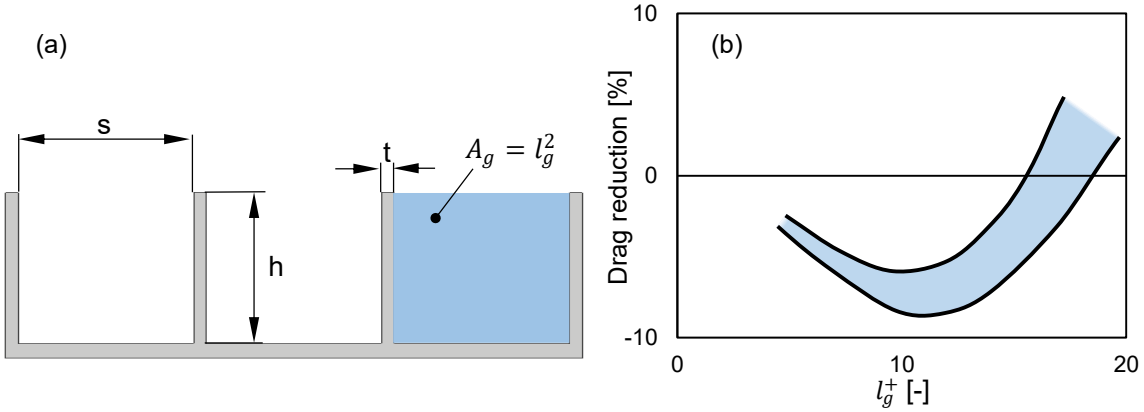

Figure 1: (a) Blade-shaped riblets with their basic dimension and (b) drag reduction range of various riblet geometries as a function of l_g^+ , adapted from (García-Mayoral and Jiménez, 2011)

The application of riblets to conventional HAWTs has been previously investigated, using both experimental and numerical methods, aiming at reducing the wind turbine blade drag and increasing their efficiency. The riblets are applied to the surface of the blades where the boundary layer has transitioned to turbulent. Riblets have been shown to improve the performance of both conventional horizontal-axis and vertical-axis wind turbines. Several studies have demonstrated that riblets can reduce the drag and increase the lift coefficient by up to 8 % and 3 % (Leitl et al., 2020) and improve the power output of wind turbines by up to 5 % (Chamorro et al.,2013). The main obstacle to using riblets in such large-scale applications is the actual size of conventional wind turbine blades (around 40-100 m long), consequently the inherent difficulty of applying the riblet geometries to the blade surface, as well as their associated manufacturing and maintenance costs. However, most of these issues are alleviated when the riblets are applied to SHWTs, which have significantly smaller dimensions (blades around 1.5-3.5 m) and reduced associated costs. The application of riblets to SHWTs is of great interest to engineers due to their relative simplicity and potentially substantial performance gain and is the primary aim of this work. More specifically, the riblet effect is implemented through a surrogate modelling method on both 2D airfoil profiles as well as the rotating, fully 3D wind turbine blade. The appropriate areas to which the riblets can be applied are initially identified, and subsequently, the performance enhancement from optimal as well as non-optimal riblets is examined by means of RANS CFD analyses. The drag reduction on the airfoil profiles, as well as the power output gain of the whole SHWT, are evaluated for both optimal and non-optimal riblet sizes.

2. Tools and Methods

2.1 Wind turbine platform

In the present work, the effect of riblet application is examined in a typical small horizontal wind turbine (SHWT) with a 3.5 m blade radius. The SHWT operates in a high-turbulence environment and at a nominal freestream velocity of 10 m/s. The corresponding operating Reynolds number range is approximately between 200,000 and 450,000, based on the SHWT's mean aerodynamic chord. The blade of the SHWT features an NREL S834 airfoil profile with different chords and incidence angles in the span direction. An important characteristic of wind turbine performance is the tip speed ratio (λ), given in Eq(1).

$$\lambda = \frac{\hat{\omega} \cdot R}{V_\infty} \tag{1}$$

Where $\hat{\omega}$ is the blade rotational speed, R is the blade radius and V_∞ is the freestream wind velocity. Based on previous studies involving the present wind turbine, the optimal operating tip speed ratio, which maximises the produced power, was identified to be 5. For all investigations in the present work, the λ is considered constant

and equal to this optimum value. Another important parameter is the power coefficient C_P which represents the actual over the theoretical maximum power output of a wind turbine for a given blade design and wind velocity. Based on the way that riblets alter the flowfield, they are implemented only on the areas of the wind turbine blade where the boundary layer has transitioned to fully turbulent. Towards that aim, the friction coefficient C_f distribution is plotted on the selected spanwise positions of the blade and the 2D airfoil profile cases. Indicatively, in Figure 2a the C_f distributions are shown for the 2D airfoil case at 0° angle of attack and the 3D blade kink airfoil section. In Figure 2b, the blade areas where riblets are applied are shown. From Figure 2a, it is observed that the boundary layer has transitioned to fully turbulent (indicated by its sudden increase and subsequent local peak value) at roughly 50 % and 65 % of the chord length for the 2D airfoil and 3D blade.

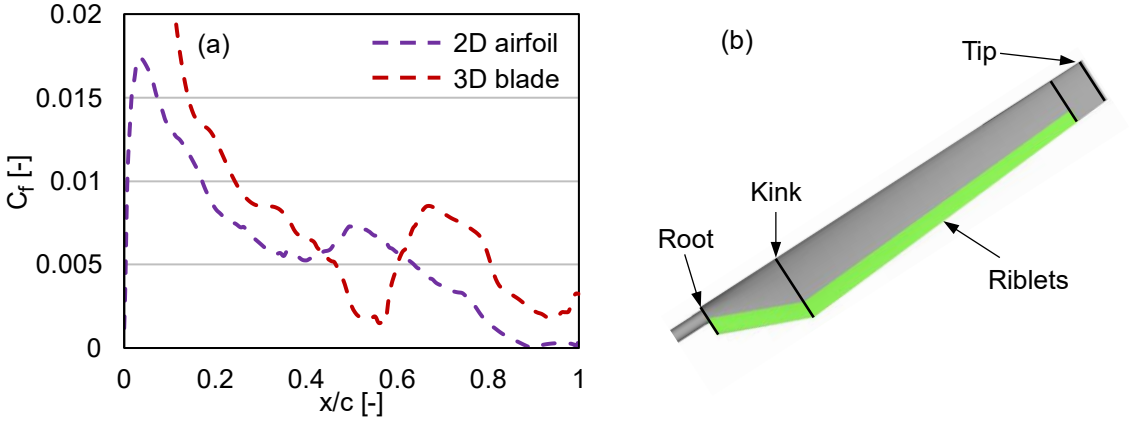

Figure 2: (a) Distribution of friction coefficient in the suction side of the airfoil and wind turbine blade, (b) and areas of riblet application on the wind turbine blade

2.2 Riblet modeling

The dimensions of riblet geometries in all engineering-related cases are several orders of magnitude smaller (in the order of ~100 μm) than the nominal dimensions of the associated problem (e.g. in SHWT, the blade radius is ~1.5-5 m). This, along with their underlying drag-reducing mechanisms, would result in the requirement of a significant computational effort for every case examined since a very fine computational mesh with gradual coarsening and high-fidelity CFD techniques (i.e. unsteady RANS and LES) are necessary.
To overcome these obstacles, Mele and Tognaccini (2012) proposed the modelling of the riblet effect as a singular roughness problem, and more specifically, by altering the original boundary condition for the specific turbulence dissipation rate *ω* (Eq(2)), in the family of k-ω turbulence models.

$$\omega = \frac{\rho \cdot u^{*2}}{\mu} \cdot S_R \tag{2}$$

The parameter S_R is only a function of the nature of the wall boundary and can be used to model the wall roughness and riblets as a function of their geometric parameters (shown in Figure 1) expressed in wall units (i.e. s^+, h^+ or l_g^+). In their work, Catalano et al. (2018) proposed an improved algebraic relationship (Eq(3)) for riblet modelling in the near-wall region, based on the non-dimensional square root of the groove cross-section l_g^+. This relationship is the result a bell type curve on the experimental data presented by Garcia-Mayoral and Jimenez (2011) and has been successfully implemented on cases related to airfoils (Bliamis et al., 2020), regional airliners (Catalano et al., 2018) and UAVs (Bliamis et al., 2022).

$$S_R = \frac{C_1}{\left(l_g^+ - C_2\right)^{2n} + C_3} \tag{3}$$

The curve fitting parameters C_1, C_2, C_3 and n are equal to 2.5×10^8, 10.5, 10^{-3} and 3.

2.3 CFD methodology

The implemented surrogate model for the riblet effect is limited to CFD computations where an ω-based turbulence model is used. In this work, the two-equation k-ω shear stress transport (SST) turbulence model is employed, along with the two-equation γ-Reθ transition model, as the most appropriate for low Reynolds number SHWT applications (Papadopoulos et al., 2020). All required computational meshes are generated using the BETA ANSA pre-processing software (v21.0.1, Root, Switzerland), are unstructured, and consist of tetra-, penta- and hexahedral cells (Figure 3a). Each unstructured computational mesh has a structured-layout region

near solid surfaces, where the boundary layer develops, with 25 cells in the normal to the wall direction (Figure 3a). The first cell height in this region is appropriately selected to ensure that everywhere the y^+ value is below unity and that at least 5 computational cells were lying within the viscous sublayer. The computational meshes used for both the 2D and 3D computations are the results of two thorough grid independence studies, using the axial and normal forces as well as produced torque (in the 3D cases) as the primary monitor variables.
The CFD analyses are performed using the ANSYS Fluent 2020R2 (Academic Multiphysics Campus Solution) software (Canonsburg, PA, USA), and, more specifically, by employing a pressure-based solver, a second-order spatial discretisation scheme for all the transport equations and the SIMPLEC scheme for the pressure-velocity coupling. In the 3D cases, a single wind turbine blade is modelled using a rotating reference frame in average operational conditions, where the wind turbine blade surface is considered stationary. To also consider the total number of blades, periodic rotational boundary conditions are applied in the two planes positioned at a 120 ° angle (Figure 3b). Finally, the freestream turbulence intensity was set equal to 5 %, a typical value for SHWT applications (Papadopoulos et al., 2020).

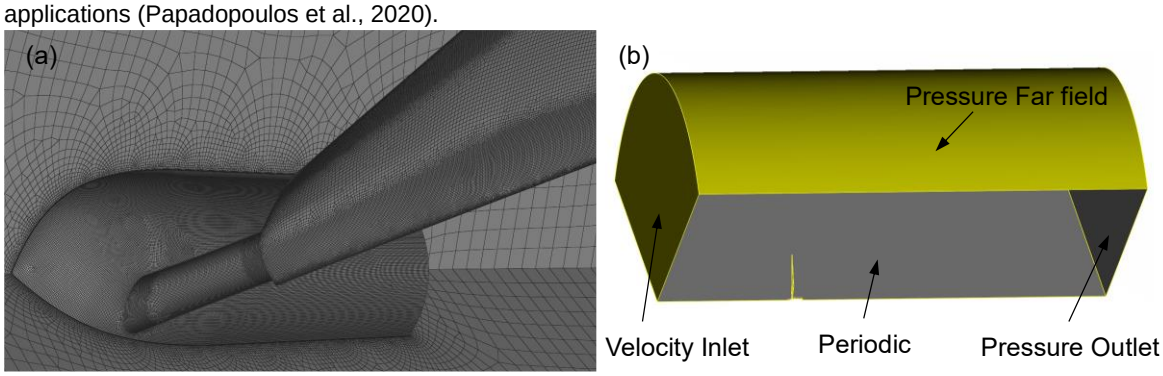

Figure 3: (a) Computational mesh on the SHWT blade and (b) boundary conditions of the control volume

3. Results

The effect of applying two different types of riblets on specific sections of the 2D airfoil and 3D blade cases is evaluated in terms of skin friction and drag reduction, as well as power coefficient enhancement. The optimal-sized riblets refer to geometries with the locally different square root of the groove cross-section (l_g) that maintain a constant l_g^+ of 10.5 and vary only due to the local wall shear stress. The averaged-sized riblets refer to geometries where the average wall shear stress (on the riblet application area) is used to calculate an average riblet sizing for the ideal l_g^+ of 10.5. The first type of riblets serves mostly as an ideal reference frame for the maximum gain that can be obtained due to its variation in sizes and difficulty to produce and apply to actual engineering problems. Contrarily, the latter type serves as the simplest solution for fabrication and application since only a single riblet size is used. However, this can result in significantly poorer performance, especially if the local wall shear values deviate largely from the mean one. More specifically, in Figure 4a, the drag reduction of the airfoil profile (given by Eq(4)) is presented in a range of AoA when applying optimal-sized and averaged-sized riblets. Since the drag-reducing mechanisms of riblets are mainly associated with the reduction of skin friction, the overall benefit is expected to be diminished as the pressure drag component becomes greater (with increasing AoA), and that is also observed for both riblet types in Figure 4a.

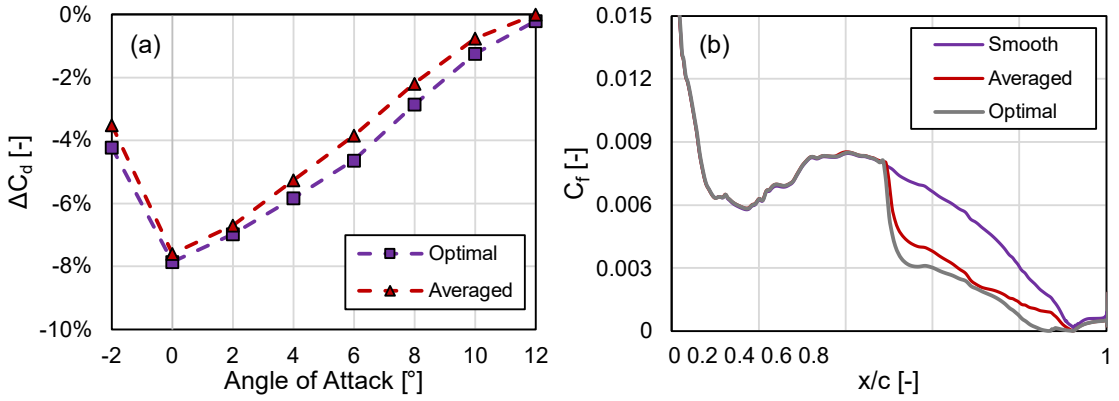

Figure 4: 2D airfoil (a) ΔC_d with optimal and averaged riblets *in the operational angle of attack range and (b) skin friction coefficient with and without riblets at 4°AoA*

$$\Delta C_d = \frac{(C_{d,smooth} - C_{d,riblets})}{C_{d,smooth}} \times 100\% \quad (4)$$

Additionally, in Figure 4b the reduction in the skin friction coefficient distribution on the airfoil profile at 4° AoA is presented. The application of riblets is evident, as downstream of the x/c=0.5 position, the skin friction is drastically reduced. The greatest effect is achieved by the optimal-sized riblets, while the average-sized riblets are also highly efficient in this particular case.

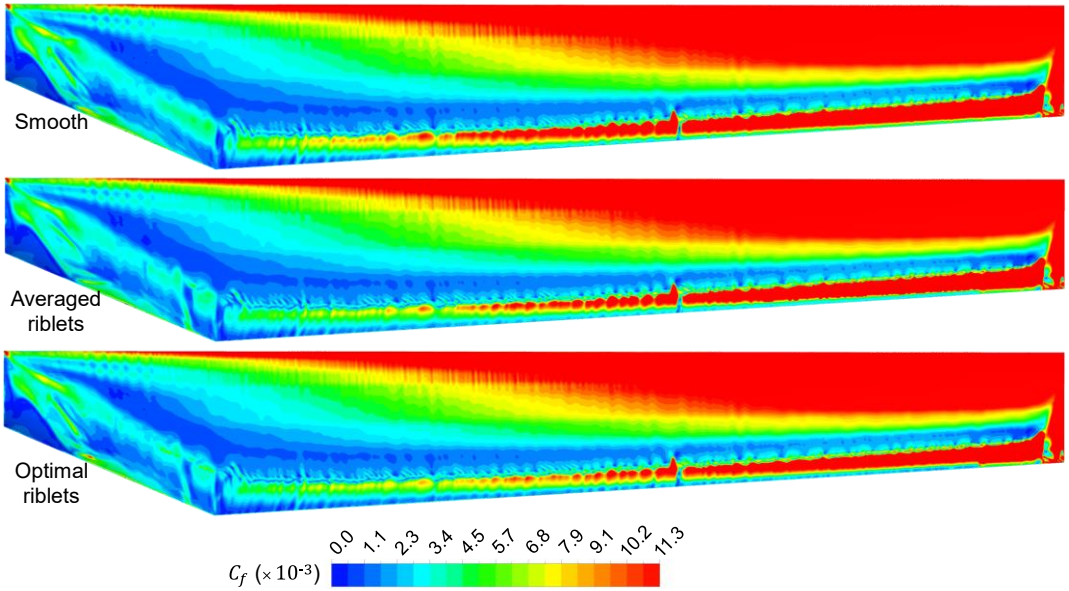

Figure 5: Skin friction distribution on the SHWT blade for smooth surface, averaged, and optimal riblet size

In Figure 5, the skin friction distributions on the 3D blade of the SHWT are presented, with and without riblet application. Similarly to the 2D cases, the optimal-sized riblets provide the greatest drag reduction. The riblets are more effective in the areas towards the blade tip and less towards the SHWT's hub. The differences in skin friction reduction between the three cases are more evident near the blade's trailing edge (indicated with dashed lines). This skin friction reduction results in a subsequent increase in the produced power from the SHWT and is presented in Figure 6, through the power coefficient.

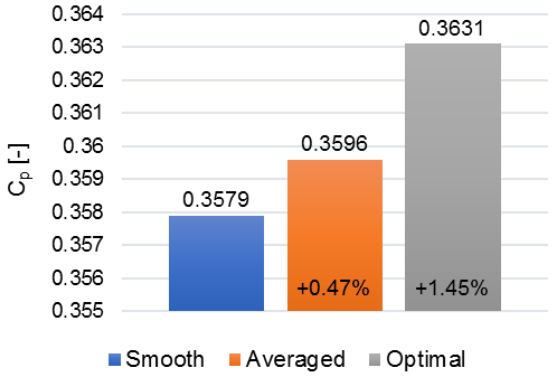

Figure 6: SHWT power coefficient improvement with and without riblet application

4. Conclusions

In this work, the application of riblets in a small horizontal wind turbine to improve its performance is investigated numerically. The effect of riblets is implemented in the regions where the flow has transitioned to fully turbulent through a surrogate model, which alters the original ω boundary condition. The modified ω values are only a function of the local l_g^+ of riblets. For the 2D airfoil, the use of riblets provides a maximum drag reduction of almost 8 % and 7.5 % for optimal- and averaged-sized riblets. The latter provide higher drag coefficients (about 0.5 % to 1 %) than their optimal-sized counterparts. The observed drag reduction is due to the alteration of skin friction distribution in the airfoil, and it decreases as the AoA is increased. Similarly, the riblet application on the overall blade results in a wind turbine performance enhancement, with a power coefficient increase of around 0. 5% for averaged and 1.5 % for optimal-sized riblets. It is observed that the riblets near the blade tip region

perform more efficiently compared to those near the hub. Concluding, the use of riblets can result in a meaningful performance gain for the SHWT, though smaller than those observed in large HAWTs, which to some extent can be related to the restricted application area.

Nomenclature

ρ – density, kg/m^3
μ – dynamic viscosity, Pa·s
u^* – friction velocity, m/s
C_1 – curve fitting parameter, -
C_2 – curve fitting parameter, -
C_3 – curve fitting parameter, -
n – exponential parameter, -
t – riblet thickness, m
h – riblet height, m
s – riblet width, m
A_g – riblet groove cross-section, m^2
l_g – square root of riblet groove cross-section, m
C_p – power coefficient, -
R – blade radius, m
λ – tip speed ratio, -
$\widehat{\omega}$ – blade rotational speed, rad/s
V_∞ – freestream wind velocity, m/s

Acknowledgments

This work was implemented within the project “RADAERO-Innovative Composite Materials for the Drag and Electromagnetic Signature Reduction for Applications in Aviation” (project code: Τ6ΥΒΠ-00042), which was financially supported by the European Regional Development Fund, Partnership Agreement for the Development Framework (2014–2020), co-funded by Greece and the European Union in the framework of the OPERATIONAL PROGRAMME: “Competitiveness, Entrepreneurship and Innovation 2014–2020 (EPAnEK)”, Nationwide Action: “Industrial Materials”.
The authors Chris Bliamis and Kyros Yakinthos are also affiliated with the UAV-iRC of the Center for Interdisciplinary Research and Innovation, Aristotle University of Thessaloniki Greece. The authors Zinon Vlahostergios and Dimitrios Misirlis are also affiliated with the Laboratory of Fluid Mechanics and Turbomachinery, Department of Mechanical Engineering, Aristotle University of Thessaloniki, Greece.

References

Bannier A., Garnier É., Sagaut P., 2015, Riblet Flow Model Based on an Extended FIK Identity. Flow Turbulence and Combustion, 95, 351–376, DOI:10.1007/s10494-015-9624-2.
Bliamis C., Vlahostergios Z., Misirlis D., Yakinthos K., 2020, Modeling Surface Riblets Skin Friction Reduction Effect with the Use of Computational Fluid Dynamics. Chemical Engineering Transactions, 81, 595-600, DOI:10.3303/CET2081100.
Bliamis C., Vlahostergios Z., Misirlis D., Yakinthos K., 2022, Numerical Evaluation of Riblet Drag Reduction on a MALE UAV. Aerospace, 9, 218, DOI:10.3390/aerospace9040218.
Catalano P., de Rosa D., Mele B., Tognaccini R., Moens F., 2018, Effects of riblets on the performances of a regional aircraft configuration in NLF conditions. AIAA Aerospace Sciences Meeting 2018, 1-16, DOI:10.2514/6.2018-1260.
Chamorro L., Arndt, R., Sotiropoulos F., 2013, Drag reduction of large wind turbine blades through riblets: Evaluation of riblet geometry and application strategies. Renewable Energy, 50, 1095–1105, DOI:10.1016/j.renene.2012.09.001.
García-Mayoral R., Jiménez J., 2011, Drag reduction by riblets. Philosophical Transactions of the Royal Society A, 369, 1412-1427, DOI:10.1098/rsta.2010.0359.
GWEC, 2022, Global wind report 2022, Global Wind Energy Council (GWEC), <gwec.net/global-wind-report-2022>, accessed 10.03.2023.
KC A., Whale, J., Urmee T., 2019, Urban wind conditions and small wind turbines in the built environment: A review. Renewable Energy, 131, 268–283, DOI:10.1016/j.renene.2018.07.050.
Klumpp S., Meinke M., Schröder W., 2010, Numerical simulation of riblet controlled spatial transition in a zero-pressure-gradient boundary layer. Flow, Turbulence and Combustion, 85 (1), 57–71, DOI:10.1007/s10494-010-9251-x.
Leitl P., Feichtinger C., Schreck S., Flanschger A., Stenzel V., Kordy H., Kowalik Y., Stuebing D., 2020, Riblet-surfaces for improvement of efficiency of wind turbines. AIAA Scitech 2020 Forum, AIAA 2020-0308, DOI:10.2514/6.2020-0308.
Mele B., Tognaccini R., 2012, Numerical simulation of riblets on airfoils and wings. 50th AIAA Aerospace Sciences Meeting including the New Horizons Forum and Aerospace Exposition, AIAA 2012-861, DOI:10.2514/6.2012-861.
Papadopoulos C., Schmid M., Kaparos P., Misirlis D., Vlahostergios Z., 2020, Numerical Analysis and Optimization of a Winglet for a Small Horizontal Wind Turbine Blade. Chemical Engineering Transactions, 81, 1321-1326, DOI:10.3303/CET2081221.